Journal of Power Sources 196 (2011) 7937–7944

Contents lists available at ScienceDirect

Journal of Power Sources

journal homepage: www.elsevier.com/locate/jpowsour

Development of a high power density 2.5 kW class solid oxide fuel cell stack

M. Yokoo, K. Mizuki*, K. Watanabe, K. Hayashi

NTT Energy and Environment Systems Laboratories, NTT Corporation, 3-1, Morinosato Wakamiya, Atsugi-shi, Kanagawa 243-0198, Japan

ARTICLE INFO

Article history:
Received 23 March 2011
Received in revised form 27 April 2011
Accepted 16 May 2011
Available online 27 May 2011

Keywords:
Solid oxide fuel cell
Cell stack
High electrical conversion efficiency
Durability

ABSTRACT

We have developed a 2.5 kW class solid oxide fuel cell stack. It is constructed by combining 70 power generation units, each of which is composed of an anode-supported planar cell and separators. The power generation unit for the 2.5 kW class stack were designed so that the height of the unit were scaled down by 2/3 of that for our conventional 1.5 kW class stack. The power generation unit for the 2.5 kW class stack provided the same output as the unit used for the conventional 1.5 kW class stack, which means that power density per unit volume of the 2.5 kW class stack was 50% greater than that of the conventional 1.5 kW class stack.

1. Introduction

A solid oxide fuel cell (SOFC) is a device that converts chemical energy to electricity with high conversion efficiency [1]. We have been developing a power generation system using an SOFC for use in our communication bases, where electricity is more important than heat as an energy source.

We have developed an SOFC that provides a very high power density [2,3]. We chose an anode-supported structure because it allows the use of a thin electrolyte, which provides a low electrical resistance. A cermet consisting of nickel oxide and scandia-alumina stabilized zirconia (SASZ) is used for the anode, which has a double-layer structure [3]. For the electrolyte, we use SASZ because of its high ionic conductivity. Furthermore, lanthanum nickel ferrite (LNF), which has a high electrical conductivity and is resistant to chromium poisoning, is used as the cathode material [4–7].

We have been developing a highly efficient and durable SOFC stack with an internal manifold structure by using our anode-supported cells [8–11]. The stacks are constructed by combining power generation units, each of which is composed of an anode supported planar cell and separators [8].

A 400 W class stack was developed in 2006 [8]. It was composed of 25 anode supported 100 mm-diameter SOFCs. The power density per unit volume was 0.14 W cm^{-3} when the current density was 0.30 A cm^{-2} and the fuel utilization was 60%. Here, dry hydrogen was used as fuel. In 2007, the stack output was increased to 1.1 kW by increasing the number of cells in a stack from 25 to 50, and the cell diameter from 100 to 120 mm [9]. Here, the power density per unit volume was kept at 0.14 W cm^{-3} since the current density was kept constant. Moreover, we developed a 1.5 kW class stack in 2008 [10]. This output was achieved by increasing the current density from 0.30 to 0.53 A cm^{-2}. By contrast, the number of cells in the stack was reduced to 40. The power density per unit volume was increased to 0.23 W cm^{-3} since the current density was increased. As seen above, we have been gradually increasing the stack output and power density per unit volume [8–10].

Since increasing power density of SOFC stack reduces heat radiation from itself, and makes the stack easier to fit in a system, researches of enhancing the power density have been actively conducted these days [11–16]. Recently, we have developed a 2.5 kW class stack with a higher power density per unit volume. The design and performance of the 2.5 kW class stack are reported in this paper.

2. Design of 2.5 kW class stack

This section describes the stack configuration and separator design for a 2.5 kW class stack. Moreover, the result of a simulation designed to check the fuel distribution in a 2.5 kW class stack is reported.

2.1. Stack configuration

We describe the configuration of a 2.5 kW class stack after outlining that of our conventional 1.5 kW class stack.

The conventional 1.5 kW class stack was constructed by combining four 10-cell sub-stacks. Here, the 10-cell sub-stacks were constructed by combining 10 power generation units, each of which

* Corresponding author. Present address: 3-1, Morinosato Wakamiya, Atsugi-shi, Kanagawa 243-0198, Japan. Tel.: +81 46 240 4111; fax: +81 46 270 2702.
E-mail address: mizuki.kotoe@lab.ntt.co.jp (K. Mizuki).

0378-7753/$ – see front matter © 2011 Elsevier B.V. All rights reserved.
doi:10.1016/j.jpowsour.2011.05.044

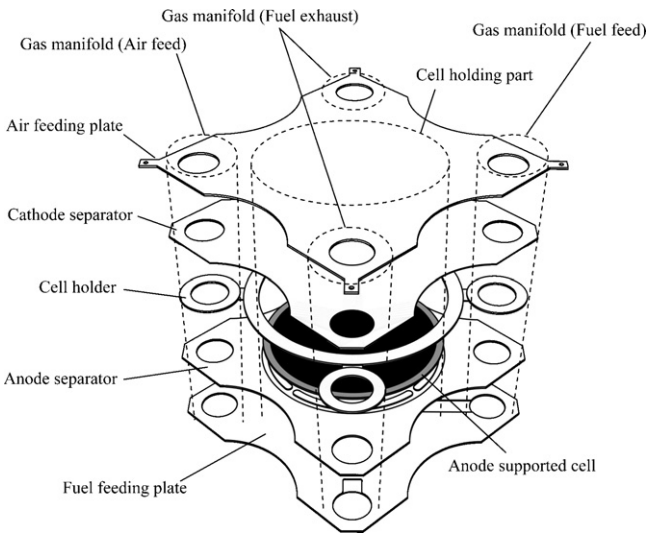

Fig. 1. Construction of power generation unit for conventional stack.

was composed of an anode supported planar cell with a diameter of 120 mm and separators as shown in Fig. 1 [8]. Plates with a thickness of 2.5 mm, which are known as intermediate plates [17], were placed at the top and bottom of the 10-cell sub-stack.

Anode supported cells 120 mm in diameter were also used in the 2.5 kW class stack. The number of cells in the stack was increased from 40 to 70 to achieve the target output of 2.5 kW. Five 14-cell sub-stacks were combined. Each 14-cell sub-stack was sandwiched between intermediate plates in the same way as the 10-cell sub-stack in the conventional 1.5 kW class stack.

2.2. Separator design

The conventional 1.5 kW class stack employs two types of feeding plates, namely a "fuel feeding plate" and an "air feeding plate", as shown in Figs. 1 and 2(a). The fuel and air move to the center of the cells from the manifold through these plates. In contrast, one type of feeding plate, called a "fuel and air feeding plate", was used in the 2.5 kW class stack as shown in Fig. 2(b). The use of this plate is expected to increase the power density per unit volume.

The thickness of the plates was designed so that height of the power generation unit for the 2.5 kW class stack was 2/3 of that for the conventional 1.5 kW class stack. Specifically, in the 2.5 kW class stack 1.0 mm thick plates were used for the anode and cathode separator, and 0.5 mm thick plates were used for the fuel and air feeding plates. Here, the fuel and air were fed to off-center points in the cell.

The diameter of the manifold in the 2.5 kW class stack was the same as that in the conventional 1.5 kW class stack.

2.3. Fuel distribution in 2.5 kW class stack

The fuel distribution in the 2.5 kW class stack was checked by employing a numerical simulation. The simulation result is shown after an explanation of the schematic diagram of the 2.5 kW class stack.

Fuel is fed from the bottom and distributed to each cell through the fuel feed manifold as shown in Fig. 3. Exhaust fuel from the cells collects in the fuel exhaust manifold and is emitted from the bottom. Although only one fuel exhaust manifold is shown in Fig. 3, the 2.5 kW class stack has two fuel exhaust manifolds (see Fig. 1). The cells were numbered from the bottom.

The simulation result is shown in Fig. 4. In this figure, the horizontal axis indicates the cell number, and the vertical axis indicates

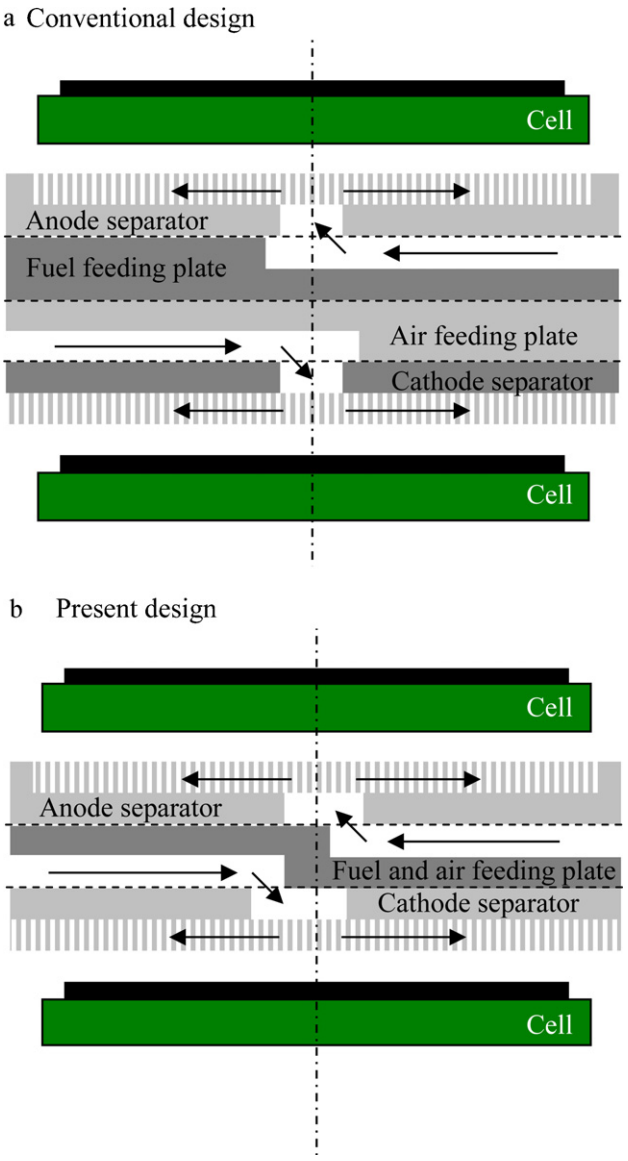

Fig. 2. Cross-section drawing of stacks: (a) Conventional design, (b) present design.

the deviation in the amount of fuel fed to each cell. Here, the deviation Δf was defined as:

$$\Delta f_i = \frac{m_i - \overline{m}}{\overline{m}} \times 100, \quad (1)$$

where, m_i is fuel amount fed to each cell, and $\overline{m}$ is the average fuel amount fed to all the cells. The average fuel amount $\overline{m}$, and the operating temperature were set at 315 ml min^{-1}(STP), and 1073 K, respectively. The simulation was carried out under open circuit conditions. For comparison, Fig. 4 also shows a simulation result for a conventional 1.5 kW class stack. A larger amount of fuel was fed to the cells with a smaller number in both stacks. This is reasonable in a laminar flow field since fuel was fed from the bottom. The deviation Δf was slightly larger for the 2.5 kW class stack than for the conventional 1.5 kW class stack. However, Δf was less than 0.2% in the 2.5 kW class stack, and we concluded that this is small enough for a uniform fuel distribution.

3. Experiment

First, the performance of a 3-cell stack with the present structure shown in Fig. 2(b) was investigated to evaluate the present

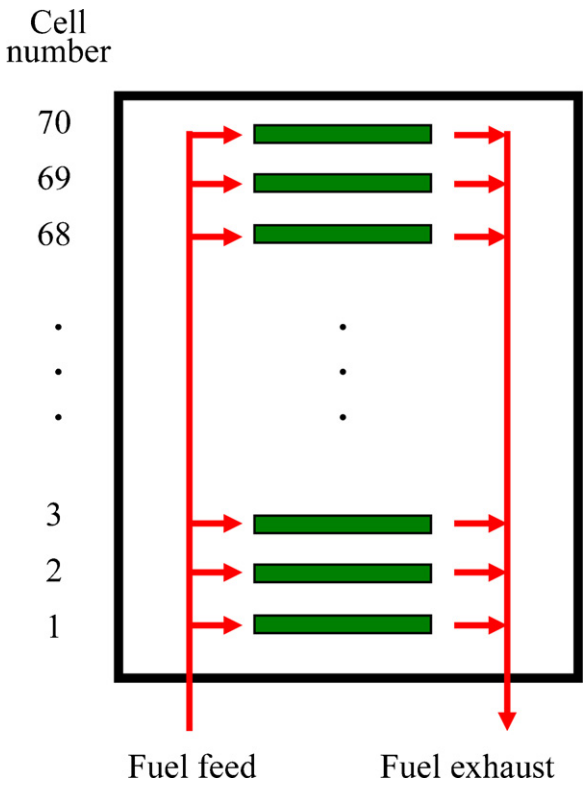

Fig. 3. Schematic diagram of 2.5 kW class stack.

design. Hereafter, a stack with the present structure is referred to as a present stack, for example a "present 3-cell stack". Then, a present 14-cell stack, which is one sub-stack of the 2.5 kW class stack, was examined. Finally, a present 70-cell (2.5 kW class) stack was constructed and evaluated. The performance of the present 3-, 14-, and 70-cell stacks is described in Sections 4.1, 4.2 and 4.3, respectively.

Dry hydrogen was used as a fuel and dry air was used as an oxidant. The stack was placed in an electric furnace. The temperature of the electric furnaces was set at 1073 K. Power generation tests were carried out after the anodes of the cells had been reduced by the hydrogen. Each cell voltage was measured as the difference between the voltages of the top and bottom of the same power generation unit (see Fig. 2). When we investigated the effect of fuel utilization on stack performance, we varied the fuel flow rate while

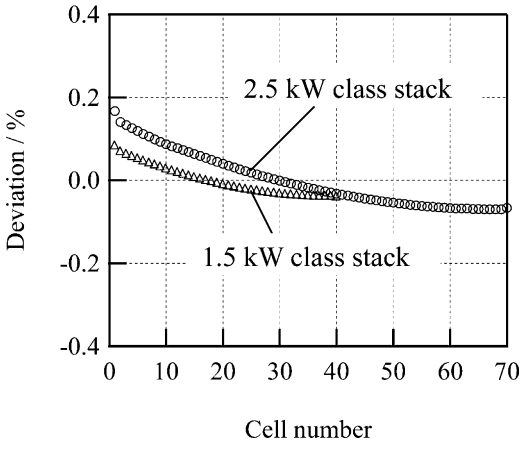

Fig. 4. Simulation results for fuel distribution in conventional 1.5 kW class and present 2.5 kW class stacks.

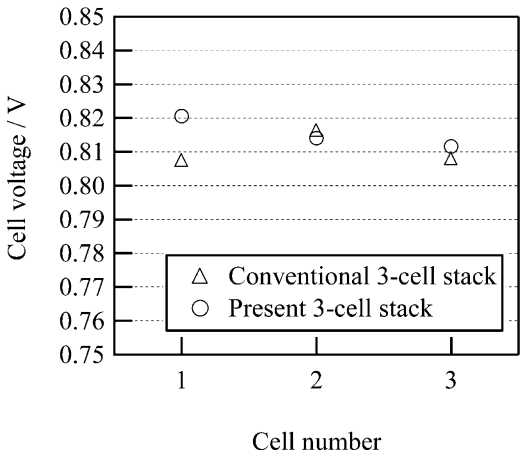

Fig. 5. Cell voltage at a current density of 0.53 A cm^{-2} and fuel utilization of 75% in conventional and present 3-cell stacks.

keeping the current density and air flow rate constant. Exhaust fuel from the stack was fed to a condenser to extract the water. The exhaust air from the stack was released into the atmosphere via a joint gap in the electric furnace.

4. Results and discussion

4.1. Performance of 3-cell stack

The initial performance of each cell in a present 3-cell stack is shown in Fig. 5. In this figure, the horizontal axis indicates the cell number and the vertical axis indicates each cell voltage at a current density of 0.53 A cm^{-2} and a fuel utilization of 75%. For comparison, Fig. 5 also shows the initial performance of a 3-cell stack with the conventional structure shown in Fig. 2(a), which is referred to as a conventional 3-cell stack. The average cell voltages were 0.815 and 0.811 V for the present and conventional 3-cell stacks, respectively. The average cell voltage was almost the same for the present and conventional 3-cell stacks. The differences between the maximum and minimum cell voltages were 9.0 and 8.9 mV for the present and conventional 3-cell stacks, respectively. The deviation of the cell voltages in a stack was almost the same for both kinds of 3-cell stacks.

The influence of fuel utilization on the cell voltage in the present 3-cell stack is shown in Fig. 6. Here, the current density was kept at 0.53 A cm^{-2}. The effect of fuel utilization on each cell voltage was

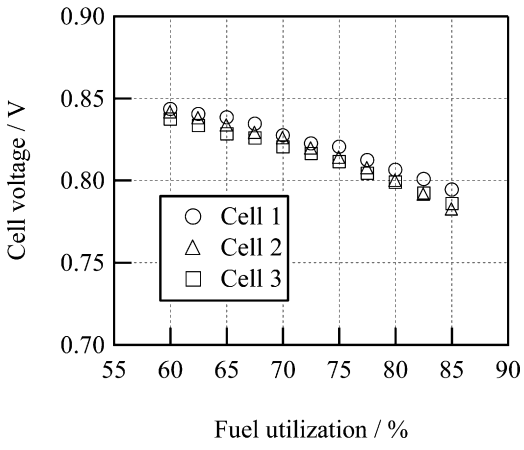

Fig. 6. Cell voltage as a function of fuel utilization at a current density of 0.53 A cm^{-2} in a present 3-cell stack.

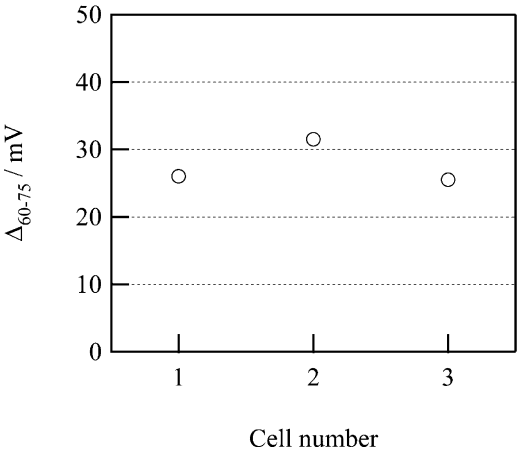

Fig. 7. Change in each cell voltage at a current density of 0.53 A cm^{-2} when the fuel utilization was changed from 60% to 75% in a present 3-cell stack.

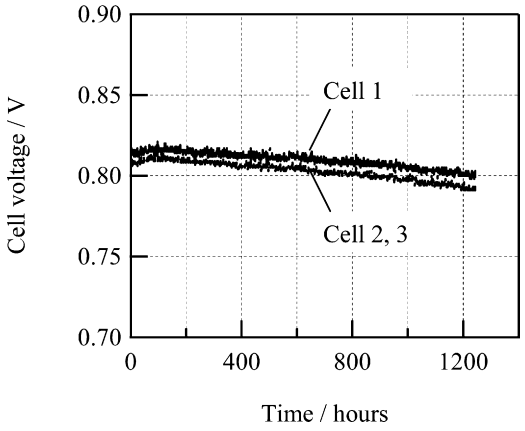

Fig. 9. Time dependence of each cell voltage at a current density of 0.53 A cm^{-2} and a fuel utilization of 75% in a present 3-cell stack.

almost the same, which means all the power generation units had almost the same fluid resistance, and so almost the same amount of fuel was fed to each cell while the total amount of fuel was varied. To discuss this in detail, we investigated the change in each cell voltage when the fuel utilization was changed from 60% to 75%. We refer to this change in cell voltage as Δ_{60-75} (=$V_{UF:60}$−$V_{UF:75}$). We think that Δ_{60-75} has a strong correlation with fuel distribution, though each cell voltage is influenced not only by fuel distribution but also by gas sealant performance and the contact resistance between the cell and the separator. Fig. 7 shows the Δ_{60-75} for each cell in the present 3-cell stack. The Δ_{60-75} for cell 2 was slightly larger than those for cells 1 and 3. This seems to be because the temperature was higher around the center of the stack than around the edge [18]. The higher temperature leads to higher fluid resistance in the power generation units. In the stacks, the effect of fuel flow rate on cell voltage is larger in a power generation unit with a higher fluid resistance. This is because a smaller amount of fuel is fed to a power generation unit with a higher fluid resistance, and effect of the fuel flow rate on cell voltage increases when the fuel flow rate decreases.

The influence of fuel utilization on the average cell voltage in the present 3-cell stack is shown in Fig. 8. For comparison, Fig. 8 also shows that in the conventional 3-cell stack. The influence was slightly larger for the present 3-cell stack. We considered this to be because, unlike with the conventional stack, the fuel is not fed strictly to the center of the cell in the present stack. This leads to a non-uniformity of the gas spread in the anode separators in the present stack. The effect of the non-uniformity of the fuel spread will be investigated by numerical simulation in the future.

The time dependence of each cell voltage in the present 3-cell stack at a current density of 0.53 A cm^{-2} and a fuel utilization of 75% is shown in Fig. 9. The difference between the maximum and minimum cell voltages was almost constant for over 1200 h. The time dependence of the average cell voltage in the present 3-cell stack is shown in Fig. 10. The figure also shows that in the conventional 3-cell stack for comparison. In both kinds of stacks, the current density and fuel utilization were kept at 0.53 A cm^{-2} and 75%, respectively. The average cell voltage in the present 3-cell stack increased in the first 100 h, and then decreased with a degradation rate of 1.90% per 1000 h. This degradation rate was larger than that in the conventional 3-cell stack, which was 0.67% per 1000 h. We consider that this is also because the fuel is not fed strictly to the center of the cell in the present 3-cell stack. Since the fuel did not spread uniformly in the anode separators in the present stack, we believe this causes the lack of fuel in certain area of electrode to cause the degradation of it. The durability should be improved.

4.2. Performance of 14-cell stack (1 sub-stack)

The initial performance of each cell in a present 14-cell stack, which is 1 sub-stack in a 70-cell stack, is shown in Fig. 11. The horizontal axis indicates the cell number and the vertical axis indicates each cell voltage at a current density of 0.53 A cm^{-2} and a fuel uti-

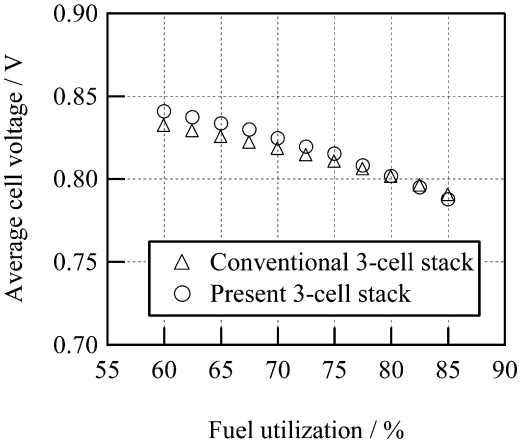

Fig. 8. Average cell voltage as a function of fuel utilization at a current density of 0.53 A cm^{-2} in conventional and present 3-cell stacks.

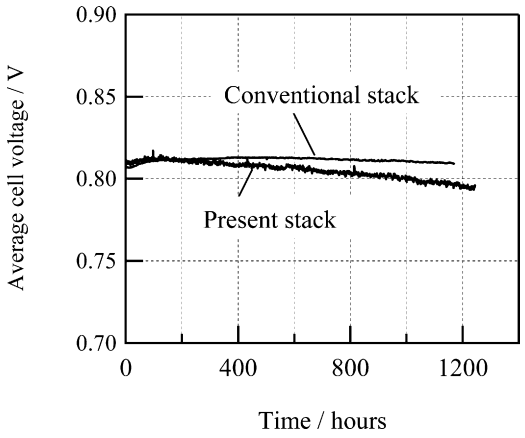

Fig. 10. Time dependence of the average cell voltages at a current density of 0.53 A cm^{-2} and a fuel utilization of 75% in conventional and present 3-cell stacks.

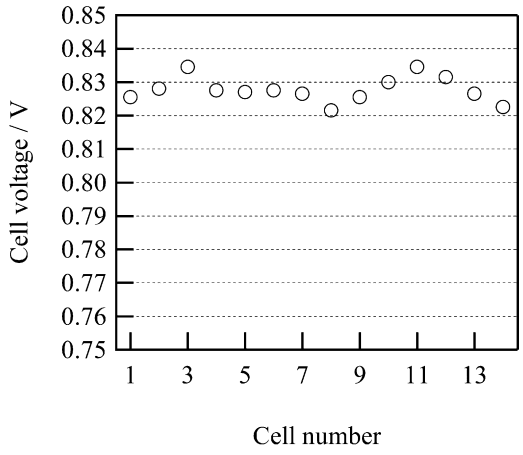

Fig. 11. Cell voltage at a current density of 0.53 A cm^{-2} and a fuel utilization of 75% in a present 14-cell stack.

lization of 75%. The deviation of the cell voltages, ΔV, was ±1.5%. Here, the deviation ΔV was defined as:

$$\Delta V_i = \frac{V_i - \overline{V}}{\overline{V}} \times 100, \quad (2)$$

where, V_i is each cell voltage, and $\overline{V}$ is the average cell voltage. The cells near the top and bottom, which have cell numbers of 1, 2 or 13, 14, and those around the center, which have cell numbers of around 7, showed slightly lower voltages. We believe this can be explained by the temperature distribution in the stack. Below, we discuss the relationship between temperature distribution and cell voltage in detail using Fig. 12. We consider that the temperature was highest at around the center as shown in Fig. 12(a). In stacks, the temperature influences both fluid resistance and electrical resistance. Specifically, the fluid resistance is proportional to 3/2 power of the temperature, and the electrical resistance is proportional to the exponent of the inverse temperature. Therefore, when the temperature distribution is as shown in Fig. 12(a), the fluid resistance is at its largest around the center as shown in Fig. 12(b), and the electric resistances of the cells are largest around the edge as shown in Fig. 12(c). Both the high fluid resistance and electrical resistance make a negative contribution to the cell voltage in the stack as mentioned below. When a power generation unit has a higher fluid resistance than its surrounding units, the cell voltage is lower since a smaller amount of fuel is fed to such a unit. We consider that the cells around center of the present 14-cell stack exhibited lower voltages for this reason. Moreover, a higher electrical resistance leads to a larger voltage drop under a constant current density condition. We consider that the cells around the edge of the present 14-cell stack exhibited a lower voltage for this reason.

The dependence of the fuel utilization on each cell voltage in the present 14-cell stack is shown in Fig. 13. In this figure, the horizontal axis indicates the cell number and vertical axis indicates the Δ_{60-75}. Here, the current density was kept at 0.53 A cm^{-2}. The figure also shows the result for the present 3-cell stack for comparison. The Δ_{60-75} range in the present 14-cell stack was from about 20–30 mV. There was no significant difference in Δ_{60-75} between the present 3- and 14-cell stacks. From this result, we concluded that the fuel distribution in the present 14-cell stack was acceptable. Δ_{60-75} was largest at the center in the present 14-cell stack. We consider this to be because the temperature was the highest there, and so the fluid resistance was also the highest there.

The time dependence of the average cell voltage in the present 14-cell is shown in Fig. 14. The figure also shows that in the present 3-cell stack for comparison. In both stacks, the current density and

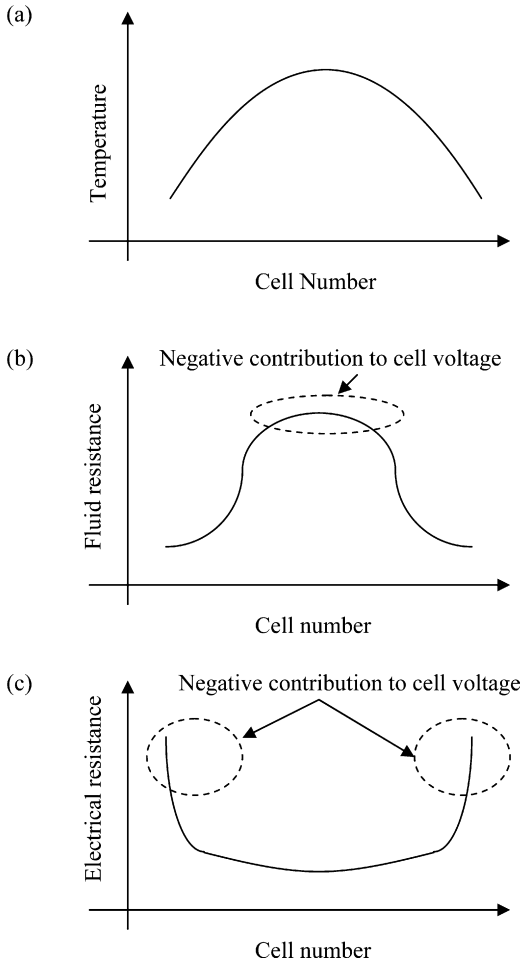

Fig. 12. Influence of temperature distribution on fluid and electrical resistance in a present 14-cell stack. (a) Temperature distribution, (b) distribution of fluid resistance, (c) distribution of electrical resistance.

fuel utilization were kept at 0.53 A cm^{-2} and 75%, respectively. The average cell voltage in the present 14-cell stack increased in the first 100 h as in the present 3-cell stack. Then it decreased with a degradation rate of 1.50% per 1000 h. This degradation rate was almost the same as that in the present 3-cell stack, which was 1.90%. We concluded that increasing number of cells did not cause significant degradation in the long-term stability.

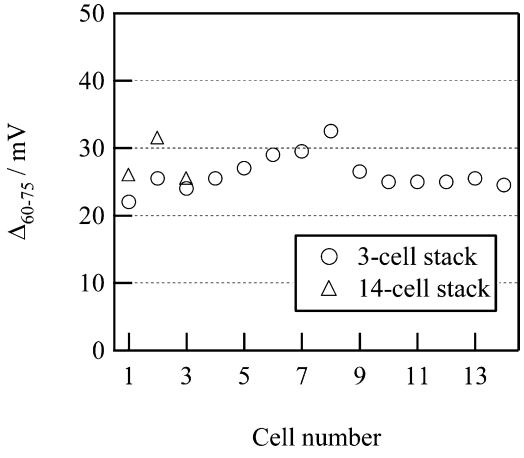

Fig. 13. Change in each cell voltage at a current density of 0.53 A cm^{-2} when the fuel utilization was changed from 60% to 75% in a present 14-cell stack.

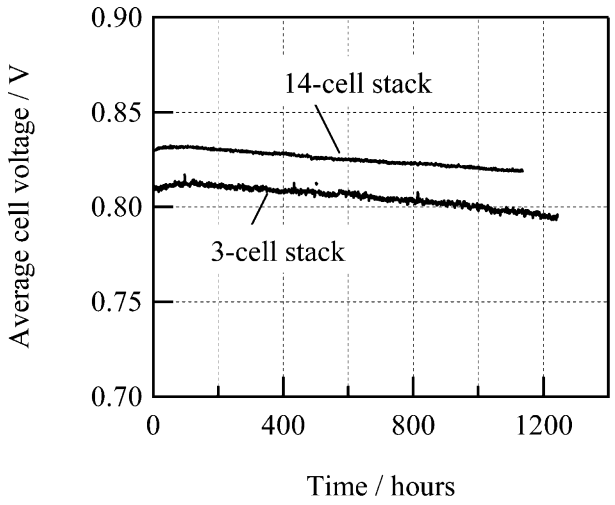

Fig. 14. Time dependence of average cell voltages at a current density of 0.53 A cm^{-2} and a fuel utilization of 75% for present 3-cell and 14-cell stacks.

Fig. 15. Present 70-cell stack (2.5 kW class stack).

4.3. Performance of 70-cell stack (2.5 kW class stack)

A present 70-cell stack was constructed by combining five 14-cell sub-stacks as shown in Fig. 15. The size of the power generation region was about 8610 cm^3.

The average cell voltage $\overline{V}$ as a function of current density in the present 70-cell stack is shown in Fig. 16. The figure also shows that in a conventional 40-cell stack for comparison. In both stacks,

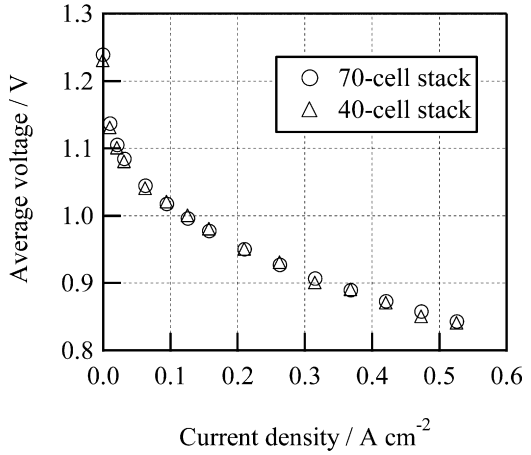

Fig. 16. Average cell voltages as a function of current density in conventional 40-cell and present 70-cell stacks.

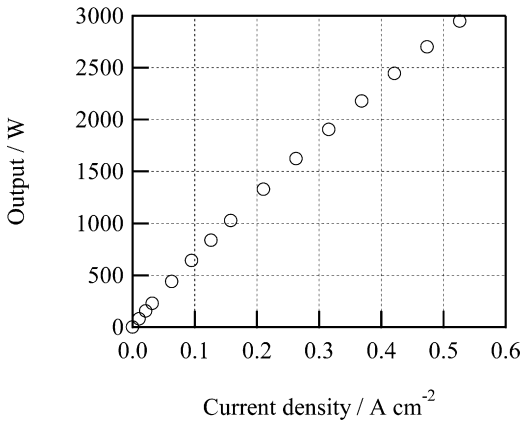

Fig. 17. Stack dc output as a function of current density in a present 70-cell stack.

the fuel amount was determined so that the fuel utilization was 60% when the current density was 0.53 A cm^{-2}. Both stacks provided almost the same $\overline{V}$ at each current density. The power density per unit volume in the present 70-cell stack was 0.34 W cm^{-3}, which is about 1.5 times that in the conventional 40-cell stack (0.23 W cm^{-3}). This is because the height of the power generation unit in the present 70-cell stack was about two thirds of that in the conventional 40-cell stack. Fig. 17 shows the output as a function of current density in the present 70-cell stack. The output of 2950 W was achieved at a current density of 0.53 A cm^{-2}. The power density per unit volume and output in our developed stacks are summarized in Fig. 18 [8–10]. These are the values obtained when the hydrogen was used as the fuel and the fuel utilization was 60%.

The stack output and electrical efficiency at gross dc as a function of fuel utilization in the present 70-cell stack is shown in Fig. 19. The fuel utilization was varied by changing the fuel flow rate, while the current density was kept at 0.53 A cm^{-2}. The stack output decreased with the fuel utilization. This is because the stack voltage decreased with the fuel utilization since the molar fraction of steam increased with the fuel utilization on the anode side. By contrast, the electrical efficiency at gross dc, which we calculated by using the LHV of the hydrogen, increased with the fuel utilization. Although the stack voltage decreased with the fuel utilization, the decrement in the amount of unused fuel led to higher electrical efficiency. The stack output and electrical efficiency were 2880 W and 49%, respectively, when the fuel utilization was 75%.

Each cell voltage at a current density of 0.53 A cm^{-2} and a fuel utilization of 75% in the present 70-cell stack is shown in Fig. 20. The deviation, ΔV, of the cell voltages was ±2.5%. The cells around the center exhibited a higher voltage than the cells around the edges. This situation is different from that in the present 14-cell stack.

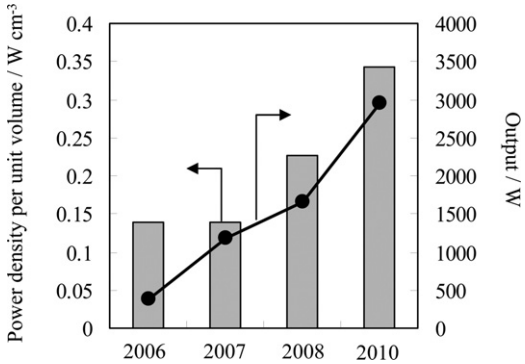

Fig. 18. Power density per unit volume and stack dc output at a fuel utilization of 60% in stacks developed in 2006, 2007, 2008, and 2010.

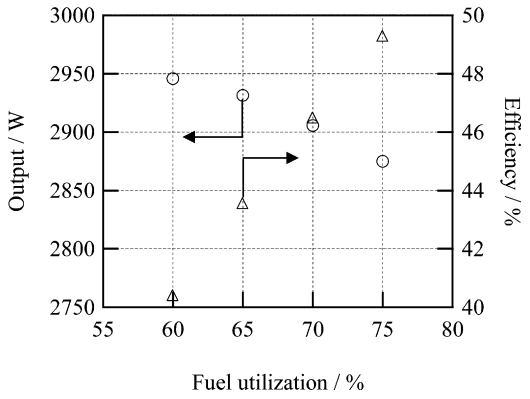

Fig. 19. Stack dc output and electrical efficiency (LHV base) at a current density of 0.53 A cm^{-2} as a function of fuel utilization in a present 70-cell stack.

However, we consider that the temperature was also at its highest around the center in the present 70-cell stack. We think that difference between the temperatures at the center and the edge, ΔT, was larger for the present 70-cell stack than for the present 14-cell stack. As mentioned above, the fluid resistance is proportional to 3/2 power of the temperature, though the electrical resistance is proportional to the exponent of the inverse temperature. We consider that the electrical resistance changed more rapidly than the fluid resistance when ΔT increased in this temperature region. So, it leads that the influence of electrical resistance on cell voltage exceeded that of fluid resistance on cell voltage.

The dependence of each cell voltage on fuel utilization in the present 70-cell stack is shown in Fig. 21. The horizontal axis indicates the cell number and the vertical axis indicates the Δ_{60-75}. Here, the current density was kept at 0.53 A cm^{-2}. The Δ_{60-75} range in the present 70-cell stack was almost the same as that in the present 14-cell stack (see Fig. 13). It was noteworthy that each 14-cell sub-stack in the present 70-cell stack had a peak Δ_{60-75} at around the center of the sub-stack. From this result, we consider that each 14-cell sub-stack had a peak temperature at around its center as shown in Fig. 22(a). Here, the temperature distribution shown in Fig. 22(a) is superposition of those shown in Fig. 22(b) and (c). We consider that the intermediate plates function as radiator plates. Although the temperature was expected to be highest at around the center of the present 70-cell stack, the Δ_{60-75} value in the 3rd 14-cell sub-stack was relatively small. We consider that this is because the average temperature of the 3rd sub-stack was the highest and so the effect of the temperature gradient in the

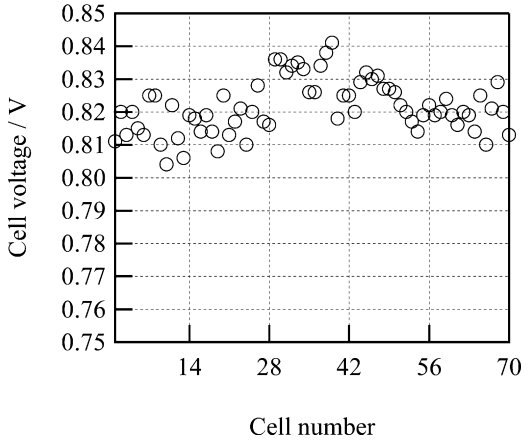

Fig. 20. Cell voltage at a current density of 0.53 A cm^{-2} and a fuel utilization of 75% in a present 70-cell stack.

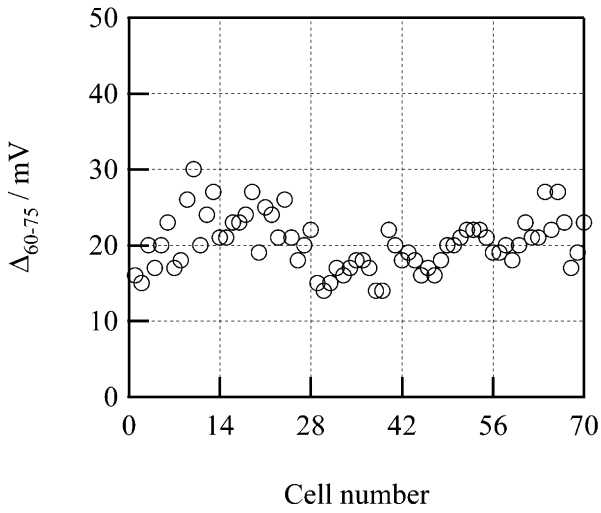

Fig. 21. Change in each cell voltage at a current density of 0.53 A cm^{-2} when the fuel utilization was changed from 60% to 75% in a present 70-cell stack.

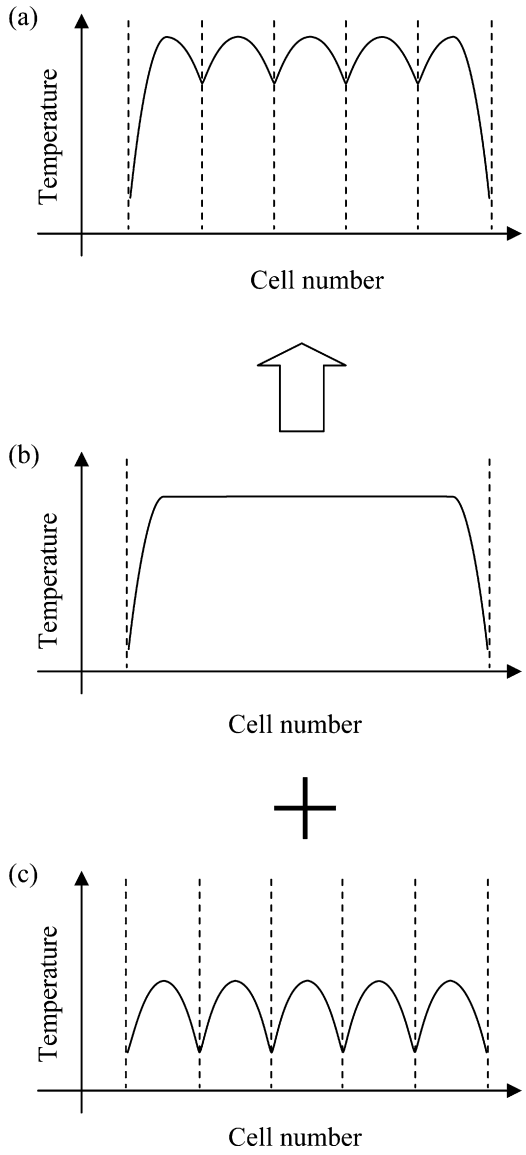

Fig. 22. Estimation of temperature distribution in a present 70-cell stack. (a) Estimated temperature distribution in a present 70-cell stack, (b) temperature distribution I, (c) temperature distribution II.

sub-stack was the smallest. Here, we expect that the difference of temperature was almost the same for all the sub-stacks.

5. Conclusion

We have developed a 2.5 kW class SOFC stack. It was constructed by combining 70 power generation units, each of which was composed of an anode-supported planar cell and separators. The separators were redesigned to increase the power density per unit volume. The power density per unit volume in the 2.5 kW class stack was 0.34 W cm^{-3}, when hydrogen was used as a fuel and the fuel utilization was 60%. This power density per unit volume is about 1.5 times that in a conventional 1.5 kW class stack. The stack output and electrical efficiency were 2880 W and 49%, respectively, when the fuel utilization was 75%. The temperature distribution in the stack was estimated by evaluating the influence of fuel utilization on each cell voltage.

References

[1] J. Larminie, A. Dicks, Fuel Cell Systems Explained, John Wiley & Sons, Ltd., 2000, pp. 207–228.
[2] H. Orui, K. Watanabe, R. Chiba, M. Arakawa, Journal of Electrochemical Society 151 (2004) A1412–A1427.
[3] H. Orui, K. Nozawa, R. Chiba, T. Komatsu, K. Watanabe, S. Sugita, H. Arai, M. Arakawa, ECS Transactions 7 (2007) 225–261.
[4] R. Chiba, F. Yoshimura, Y. Sakurai, Solid State Ionics 124 (1999) 281–288.
[5] T. Komatsu, H. Arai, R. Chiba, K. Nozawa, M. Arakawa, K. Sato, Electrochemical and Solid State Letters 9 (2006) A9–A12.
[6] T. Komatsu, H. Arai, R. Chiba, K. Nozawa, M. Arakawa, K. Sato, Journal of Electrochemical Society 154 (2007) B379–B382.
[7] R. Chiba, H. Orui, T. Komatsu, Y. Tabata, K. Nozawa, H. Arai, M. Arakawa, K. Sato, ECS Transactions 7 (2007) 1191–1200.
[8] M. Yokoo, Y. Tabata, Y. Yoshida, K. Hayashi, K. Nozawa, Y. Nozaki, H. Arai, Journal of Power Source 178/1 (2008) 59–63.
[9] M. Yokoo, Y. Tabata, Y. Yoshida, H. Orui, K. Hayashi, Y. Nozaki, K. Nozawa, H. Arai, Journal of Power Source 184/1 (2008) 84–89.
[10] K. Hayashi, M. Yokoo, Y. Yoshida, Y. Tabata, H. Orui, K. Nozawa, Y. Nozaki, H. Arai, ECS Transactions 17 (1) (2009) 53–61.
[11] D. Nishijima, et al., ECS Transactions 25 (2) (2009) 91–96.
[12] Subhasish Mukerjee, et al., ECS Transactions 25 (2) (2009) 59–63.
[13] Ellen Sun, et al., ECS Transactions 25 (2) (2009) 77–84.
[14] N. Erikstrup, et al., ECS Transactions 25 (2) (2009) 207–212.
[15] P. Szabo, et al., ECS Transactions 25 (2) (2009) 175–185.
[16] H. Arai, et al., ECS Transactions 25 (2) (2009) 125–132.
[17] M. Yokoo, Y. Tabata, Y. Yoshida, K. Hayashi, Y. Nozaki, K. Nozawa, H. Arai, Journal of Power Source 190/2 (2009) 252–257.
[18] T. Akbay, N. Chitose, T. Miyazawa, M. Shibata, F. Nishiwaki, T. Inagaki, Journal of Fuel Cell Science and Technology 6 (2009) 041007-1–041007-6.